Turbulence Characteristics in Free Surface Shear Flows

AUTHOR(S):

IMAMOTO, Hirotake

CITATION:

IMAMOTO, Hirotake. Turbulence Characteristics in Free Surface Shear Flows. Bulletin of the Disaster Prevention Research Institute 1973, 22(3): 153-186

ISSUE DATE:

1973-03

URL:

http://hdl.handle.net/2433/124828

Bull. Disas. Prev. Res. Inst., Kyoto Univ., Vol. 22, Part 3, No.205, March. 1973

Turbulence Characteristics in Free Surface Shear Flows

by Hirotake IMAMOTO

(Received Feb. 28, 1973)

Abstract

The Eulerian and the Lagrangian characteristics of turbulence in a two-dimensional free surface shear flow are investigated both theoretically and experimentally. Using the Kolmogorov's similarity theory, a whole aspect of one-dimensional turbulence energy spectrum can be determined by the two among three fundamental turbulence parameters, that is, the turbulence intensity, the Eulerian integral scale and the energy dissipation rate, and by the kinematic viscosity of fluid. Some turbulence parameters may be expressed in forms of universal function dependent on the relative depth alone, through the Reynolds number similarity.

The experimental results of probability distribution show that the Gaussian distribution can not always be applied for the turbulent velocity in a free surface shear flow, and the characteristics of probability distribution may be explained qualitatively by the effect of an intermittent violent motion generated near the channel bed. The power law of -5/3 for the Eulerian spectrum and of -2 for the Lagrangian spectrum are verified through laboratory experiments, and the specific forms of universal function for the turbulence intensity, the Eulerian integral scale and the energy dissipation rate are also determined.

1. Introductory Statement

After the statistical theory of turbulence was introduced by Taylor,[1),2)] the characteristics of turbulence in various fields have been investigated both theoretically and experimentally by many researchers.[3)] In the field of hydraulic engineering, many practical problems, such as the diffusion or the dispersion of waste waters and the transport of sediment, depend on turbulent motion. However, there is little information concerning the turbulence characteristics in open channel flows because of the deficiency of a suitable instrument for water flows.

Many methods and instruments have been tried for the investigation of water turbulence. These include the total head tube,[4)] the propeller-type current meter,[5),6)] the hot-film flowmeter,[7),8)] the ultrasonic flowmeter,[9)] the electrokinetic transducer[10)] and so on. Each of them can not satisfy perfectly the conditions of stability, responsibility, linearity, directional resolvability of velocity vector, simplicity of handling, and low cost. Therefore, the practice of turbulence measurements in open channel flow has been limited to controlled and simplified conditions.

This paper deals with the Eulerian and the Lagrangian turbulence characteristics in a two-dimensional free surface shear flow. In Section 2, using the Kolmogorov's similarity theory which has been applied to various fields of turbulence, a whole aspect of Eulerian one-dimensional wave-number spectrum is characterized by the two among three fundamental parameters, that is, the turbulence intensity, the

Eulerian integral scale and the energy dissipation rate. In Section 3, these parameters may be described in forms of universal function by the application of the Reynolds number similarity, and the specific forms of universal function will be proposed through theoretical and dimensional considerations. Section 4 deals with the statistical effects of finite evaluating time for turbulence parameters, which will be important in the practice of turbulence measurements.

The Eulerian measurements of turbulence in free surface shear flows were carried out with a hot-film anemometer in the laboratory channel and with a propeller-dynamo current meter in the field canal, while the Lagrangian measurements were made by the tracking of floating particle-tracers on the free surface. The results obtained are summarized in Section 5. The Eulerian wave-number spectrum, which may be replaced by the frequency spectrum under the assumption of frozen turbulence, will be expressed by $-5/3$ power law in the inertial sub-range, while the Lagrangian frequency spectrum will be expressed by -2 power law. Furthermore, the specific forms of universal function for the turbulence intensity, the Eulerian integral scale and the energy dissipation rate will be determined.

Some of the results in this paper have been published previously by the author.[11),12),13)]

2. Basic Characteristics of Turbulence Spectrum

2.1 Kolmogorov's Similarity Theory

The Eulerian space-correlation coefficient $R(x)$ between the turbulent velocities at two points apart a distance x is defined as

$$R(x)=\overline{u(x_0)\ u(x_0+x)}\ /\ \overline{u^2} \tag{2.1}$$

and the Eulerian integral scale L, which was suggested by Taylor[2)] as a possible definition of the average size of eddies, is given by

$$L=\int_0^\infty R(x)\,dx \tag{2.2}$$

provided that the integral converges. The assumption of homogeneity is implied in these expressions.

The Eulerian one-dimensional wave-number spectrum, $S(k)$, which shows how the average power of turbulent velocity is distributed over wave-numbers, is given by the Fourier transform of the space-correlation coefficient, so that

$$S(k)=\frac{2\overline{u^2}}{\pi}\int_0^\infty R(x)\cos kx\ dx \tag{2.3}$$

When k is much smaller than $2\pi/L$, it follows from Eqs. (2.2) and (2.3)

$$S(k)=\frac{2}{\pi}\overline{u^2}L \qquad \text{for } 0\leq k\ll 2\pi/L \tag{2.4}$$

This expression means that there exists the wave-number range in which the one-

dimensional spectrum is independent on k. Such range is referred to as the energy containing range or the energy production range.

For the range of high wave-numbers, the hypothesis of Kolmogorov's similarity theory [14),15),16)] may be applied under the condition of a sufficiently high Reynolds number and the spectrum will be obtained from dimensional considerations, then

$$S(k)=S_\epsilon \epsilon^{2/3}k^{-5/3} \qquad \text{for } 2\pi/L \ll k \ll 2\pi/l \tag{2.5}$$

in which S_ϵ ; a universal constant, ϵ; the turbulence energy dissipation rate per unit mass and time, l ; Kolmogorov's local scale, defined by

$$l=(\nu^3/\epsilon)^{1/4} \tag{2.6}$$

and ν is the kinematic viscosity of fluid. This range is referred to as the inertial sub-range, in which the average properties of turbulence are determined by the quantity ϵ alone. Strictly speaking, the expression of Eq. (2.5) can not be applied to one-dimensional spectrum but to three-dimensional spectrum, although this equation is broadly used as an approximate expression.[17)]

The viscosity effect becomes predominant for the range of sufficiently high wave-numbers, referred to as the range of viscous dissipation, and the average properties of turbulence are determined uniquely by the quantities of ϵ and ν. In this range, the dimensional analysis is not deterministic and produces various forms of spectra, for example,

$$S(k)=S_\nu(\epsilon/\nu)k^{-3} \qquad \text{for } k \gg 2\pi/l \tag{2.7}$$

and/or

$$S(k)=S'_\nu(\epsilon^2/\nu^4)k^{-7} \qquad \text{for } k \gg 2\pi/l \tag{2.7'}$$

in which S_ν and S'_ν are universal constants. Eq. (2.7) is consistent with the result of Inoue,[18)] while the expression of Eq. (2.7') is similar to that of Heisenberg.[19)]

Fig. 2-1 shows an outline of the Eulerian one-dimensional wave-number spectrum using a log-log plot. It may be understood from this figure that each of the spectra in three ranges described above will be approximated by a power law. The transition wave-numbers, k_L from the production to the inertial range and k_l from the inertial to the viscous range, are obtained from the combination of Eqs. (2.5), (2.6) and (2.7), so that

$$k_L=\left(\frac{\pi S_\epsilon}{2}\right)^{3/5}\left(\frac{L\epsilon}{u'^3}\right)^{2/5}L^{-1} \tag{2.8}$$

$$k_l=\left(\frac{S_\nu}{S_\epsilon}\right)^{3/4}l^{-1} \tag{2.9}$$

in which $u'=(\overline{u^2})^{1/2}$. In Eq. (2.8), assuming that

$$\epsilon=C\frac{u'^3}{L} \tag{2.10}$$

in which C is a universal constant, k_L will be inversely proportional to L, and $k_L L$

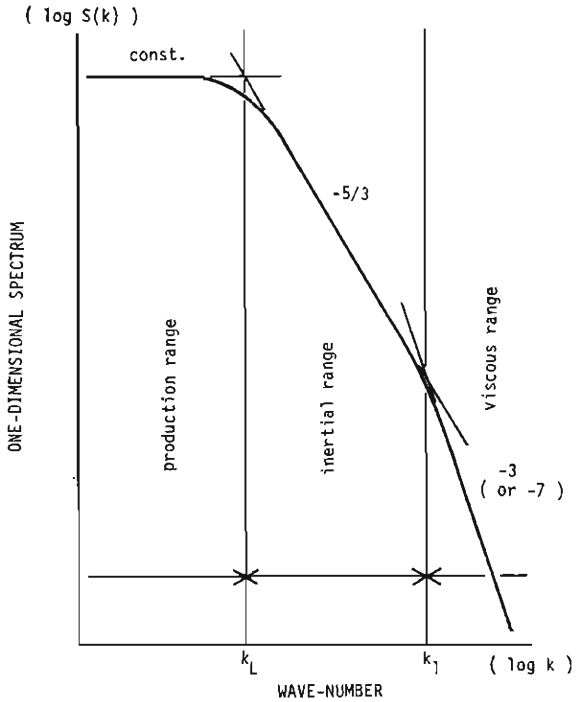

Fig. 2-1 Schematic illustration of the Eulerian one-dimensional wave-number spectrum (for uni-structural turbulence).

proportional to $\overline{u^2}$, respectively. This fact means that the property of turbulence energy production may be characterized by the quantities of length-scale L and energy-magnitude $\overline{u^2}$.

On the other hand, the Lagrangian frequency spectrum $S_L(f)$ may be obtained from the similar consideration, so that

$$S_L(f)=4\overline{u^2}T_L \qquad \text{for } 0\leq f\ll 1/T_L \tag{2.11}$$

$$S_L(f)=S_{L\epsilon}\epsilon f^{-2} \qquad \text{for } 1/T_L\ll f\ll 1/t_L \tag{2.12}$$

$$S_L(f)=S_{L\nu}(\epsilon^3/\nu)^{1/2}f^{-3} \qquad \text{for } f\gg 1/t_L \tag{2.13}$$

in which $S_{L\epsilon}$ and $S_{L\nu}$; universal constants, T_L; the Lagrangian integral time-scale, and t_L; the Lagrangian dissipation time-scale, defined as

$$t_L=(\nu/\epsilon)^{1/2} \tag{2.14}$$

The transition frequencies f_{TL} and f_{tL}, similar to k_L and k_l, will be

$$f_{TL}=\left(\frac{S_{L\epsilon}}{4}\right)^{1/2}\left(\frac{\epsilon T_L}{\overline{u^2}}\right)^{1/2}T_L^{-1} \tag{2.15}$$

$$f_{tL}=\left(\frac{S_{L\nu}}{S_{L\epsilon}}\right)t_L^{-1} \tag{2.16}$$

in which $\epsilon T_L/\overline{u^2}$ in Eq. (2.15) may be replaced by a universal constant.

It should be noticed that the Lagrangian frequency spectrum in the inertial sub-range is described by -2 power law, while the Eulerian wave-number spectrum in that range by -5/3 power law.

2.2 Spectrum of Multi-Structural Turbulence

As already examined in the atmospheric[20] and the oceanic[21] turbulence, the structure of the turbulence in a natural river may be characterized by various factors, to which, for example, the depth and the width of flow, the length-scale of sand-waves on the river bed, the radius of meandering and so on, will be suggested. The turbulence will be "multi-structural" when the effects of these factors are comparable, and will be "uni-structural" when the effect of any single factor is predominant and others are negligible. Therefore, some considerations should be necessary to extract the turbulence characteristics corresponding to the certain factor from the overall features of multi-structural turbulence.

For simplicity, consider a tripple-structural turbulence in which the turbulence energy production is characterized by three kinds of length-scale and of energy-magnitude. Then the overall turbulence spectrum is expressed as (see Fig.2-2)

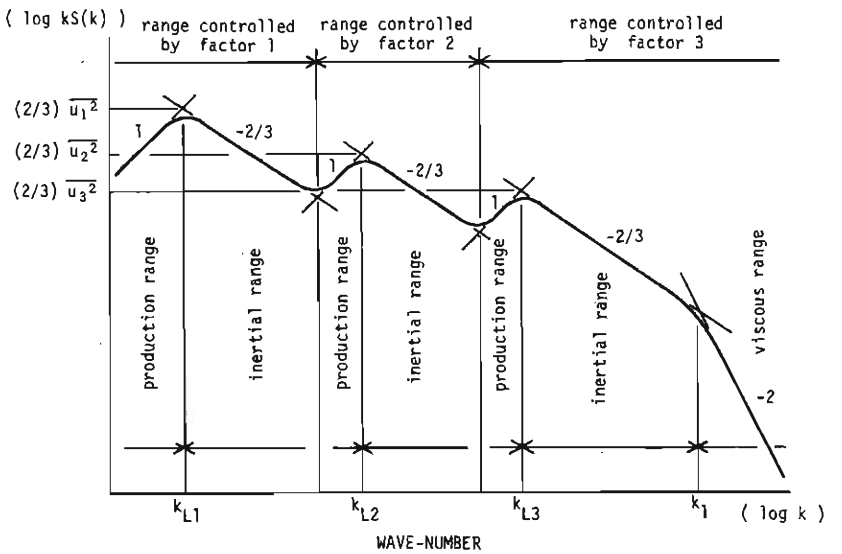

Fig. 2-2 Schematic illustration of the Eulerian one-dimensional wave-number spectrum for multi-structural turbulence.

$$S(k)=S_1(k)+S_2(k)+S_3(k)$$

in which subscripts are referred to each factor. It may be assumed that each spectrum has own properties as described in 2.1. Then, the following conditions should be satisfied in order to extract the turbulence characteristics corresponding to the factor 2,

$$\frac{\overline{u_1^2}}{\overline{u_2^2}}\left(\frac{k_{L1}}{k_{L2}}\right)^{2\cdot 3}\ll 1 \quad \text{and} \quad \frac{\overline{u_3^2}}{\overline{u_2^2}}\left(\frac{k_{L2}}{k_{L3}}\right)\ll 1 \tag{2.17}$$

For a uniform flow in a rectangular open channel, two factors of the depth and the width are essentially nominated as the characterizing factors of the turbulence field. Denoting the turbulence characteristics corresponding to the depth by the addition of subscript H and to the width by B, k_{LH} will be then proportional to the reciprocal value of H, and k_{LB} to that of B, respectively. When k_{LB} is sufficiently small compared to k_{LH}, the spectrum, whose energy production is characterized by H and $\overline{u_H^2}$, can be separated from that characterized by B and $\overline{u_B^2}$, and the following procedure will be proposed to extract the quantities of $\overline{u_H^2}$, k_{LH} and ϵ_H.

Assuming the following simple form[22] for the Eulerian one-dimensional wave-number spectrum

$$S(k)=\frac{2}{\pi}\frac{\overline{u^2}L}{(1+3Lk/\pi)^{5/3}} \tag{2.18}$$

then, the abscissa of the intersection of two asymptotic spectra on a log-log plot, that is, the transition wave-number k_L from the production to the inertial range, becomes (see Fig.2-2)

$$k_L=\frac{\pi}{3}L^{-1} \tag{2.19}$$

and the ordinate of the intersection becomes

$$[k_L S(k_L)]=\frac{2}{3}\overline{u^2} \tag{2.20}$$

Therefore, if the power laws of 1 and -2/3 are possibly applied to the production and the inertial ranges of $kS(k)$ characterized by H and $\overline{u_H^2}$, L_H and $\overline{u_H^2}$ will be determined from the abscissa and the ordinate of the intersection of two spectra, respectively. The energy dissipation rate will be obtained from the spectrum in the inertial sub-range, or from Eq. (2.10) with the values of L_H and $\overline{u_H^2}$ determined above, in which the universal constant C becomes from Eqs. (2.8), (2.10) and (2.19) to be

$$C=\frac{\pi}{3}\left(\frac{2}{3S_\epsilon}\right)^{3/2} \tag{2.21}$$

This procedure can not be applied when the width-depth ratio is not so large, and furthermore the value of C depends on the form of turbulence spectrum adopted.

2.3 Frequency Spectrum

When the velocity is measured at a fixed point, the Eulerian time-correlation cofficient $R(t)$, usually referred to as the auto-correlation coefficient, is defined by the similar manner to the space-correlation coefficient. And the Eulerian one-dimensional frequency spectrum $S(f)$ is given by the Fourier transform of $R(t)$, that is

$$S(f)=4\overline{u^2}\int_0^\infty R(t)\cos 2\pi f t\, dt \tag{2.22}$$

in which f is expressed in cycles per unit time.

$S(f)$ is related to the wave-number spectrum $S(k)$ as

$$S(f)=S(k)\ dk/df \tag{2.23}$$

in which k is expressed in radians per unit length.

The phase velocity U_p will be defined as

$$U_p=2\pi f/k \tag{2.24}$$

When $S(f)$, $S(k)$ and U_p are expressed as

$$S(f)\sim f^a,\ S(k)\sim k^b,\ \text{and } U_p(f)\sim f^\alpha \text{ or } U_p(k)\sim k^\beta \tag{2.25}$$

in which a, b and α or β are constants, and $\alpha\neq 1$, $\beta\neq -1$, it follows from Eqs. (2.23) and (2.24) that

$$\alpha=\frac{b-a}{b+1} \quad \text{or} \quad \beta=\frac{b-a}{a+1} \tag{2.26}$$

Under the assumption of frozen turbulence, the time-correlation coefficient $R(t)$ is equal to the space-correlation coefficient $R(x)$ when $t=x/U$, in which U is the mean velocity, then

$$S(f)=\frac{2\pi}{U}S(k) \quad \text{and} \quad f=\frac{U}{2\pi}k \tag{2.27}$$

Eq. (2.27) shows that there is a linear relationship between wave-number and frequency, and that the phase velocity is equal to the mean velocity independent of a wave-number or a frequency.

Using the spectrum characteristics expressed by Ogura[23] and Gifford[24] for a perfect non-frozen turbulence, that is

$$S(f)\sim f^{-2} \quad \text{and} \quad S(k)\sim k^{-5/3} \tag{2.28}$$

the phase velocity becomes

$$U_p(f)\sim f^{-1/2} \quad \text{or} \quad U_p(k)\sim k^{-1/3} \tag{2.29}$$

which means that a large-scale turbulence is convected faster than a small-scale one. This is the extreme case in which the turbulent velocity is much larger than the mean velocity. Usually, the turbulent velocity in open channel flow is smaller than the mean velocity and the assumption of frozen turbulence will hold approximately.

Hino[25] has obtained the spectrum of sand-waves in the equilibrium range with the similar method described above. That is, using -3 power law for wave-number spectrum deduced from dimensional considerations, he has obtained -2 power law for frequency spectrum in the equilibrium range through the assumption for the phase velocity, $U_p(k)\sim k^{-1}$. Adopting the law of $U_p(k)\sim k^{-1/2}$, which has been examined by Ashida[26] and Squarer,[27] the above -2 power law for frequency spectrum will be replaced by -7/3 power law. Since the difference of these expressions is very little, it is difficult to determine the superiority of each expression exprimentally.

3. Description of Turbulence Characteristics in Forms of Universal Function

3.1 Principle of Reynolds Number Similarity

It is well known as the principle of Reynolds number similarity that geometrically similar turbulent flows are similar at all sufficiently high Reynolds numbers.[28] In the case of a free surface turbulent shear flow, the whole flow can not be independent of the fluid viscosity because of the existence of a viscous sublayer, and the principle of Reynolds number similarity can only be applied to the fully turbulent region of the flow, over which the direct action of the viscosity on the mean flow is negligible. Within this region, the mean and the turbulent motions are determined by the boundary condition of the flow alone, and are independent of the fluid viscosity.

Applying the principle of Reynolds number similarity to a two-dimensional free surface turbulent shear flow, the characteristics of the mean and the turbulent motion are normalized by the representative quantities of geometric and boundary conditions, that is, the depth and the friction velocity, and the distributions of them may be expressed as universal functions of the normalized depth. For instance, the vertical profiles of the local mean velocity and the local mean shear stress, in which the Reynolds stresses are large compared with the mean viscous stresses, are expressed from this principle as

$$\frac{U_h - U}{U_f} = \phi_U\left(\frac{z}{H}\right) \tag{3.1}$$

$$\frac{\tau}{U_f^2} = -\rho\frac{\overline{uw}}{U_f^2} = \phi_\tau\left(\frac{z}{H}\right) \tag{3.2}$$

in which H ; the depth of flow, z ; the upward distance from the channel bed, u, w ; two components of the velocity fluctuation in the longitudinal and the vertical directions, U_f ; the friction velocity, U ; the local mean velocity at $z=z$, U_h ; that at $z=H$, τ ; the turbulent shear stress, ρ ; the fluid density, and ϕ ; the universal fuction of z/H alone. Two subscripts of U and τ in ϕ are referring to the mean velocity and the shear stress, respectively.

3.2 Universal Functions of Turbulence Characteristics

Various forms of universal functions for turbulence characteristics have been proposed by many researchers, and some of them have been verified by experimental investigations. The following relations are accepted as simple and general ones.

Turbulence Intensity : Usually the turbulence intensity is normalized by the friction velocity alone, then the universal function for the turbulence intensity becomes

$$\frac{u'}{U_f} = \phi_{u'}\left(\frac{z}{H}\right) \tag{3.3}$$

This expression corresponds to the principle of Monin-Obukhov's similarity,[29] which was introduced originally for the vertical component of turbulent velocity in the atmosphere.

Eulerian Integral Scale : It is implied from the dimensional consideration by Enge-

lund[30] and the hypothesis of frozen turbulence that the normalizing quantities for the Eulerian integral scale L may be $H(U/U_f)$, so that

$$\frac{L}{H(U/U_f)} = \phi_L\left(\frac{z}{H}\right) \tag{3.4}$$

Energy Dissipation Rate : Using Eqs. (3.1) and (3.2), the energy production rate by turbulent shear stress in a two-dimensional free surface shear flow is expressed in the following form of a universal function

$$[\text{energy production rate}] = -\overline{uw}\frac{dU}{dz} = \frac{U_f^3}{H}\phi_p\left(\frac{z}{H}\right) \tag{3.5}$$

Through the physical analogy of the turbulence energy production, the energy dissipation rate ϵ will be given by

$$\frac{\epsilon}{U_f^3/H} = \phi_\epsilon\left(\frac{z}{H}\right) \tag{3.6}$$

As already assumed in Eq. (2.10), ϵ is related to $\overline{u^2}$ and L by

$$\epsilon = C\frac{u'^3}{L} \tag{3.7}$$

The combination of Eqs. (3.3), (3.4) and (3.6) will establish Eq. (3.7), if all the physical assumptions involved are valid. The resultant expression, however, is of similar but a little different form. The validity of the physical significance underlying in all the descriptions should be examined through experiments. To proceed the examination, two among three expressions will be prerequestly given, and the last one will be then obtained. Three kinds of the total sequence will result, which will be listed in Table 3-1.

Other turbulence characteristics listed in Table 3-1 are derived from expressions of u', L and ϵ by means of the following relations.

From the analogy of isotropic turbulence, Taylor's dissipation scale λ is given by[2]

$$\epsilon = 15\nu\frac{\overline{u^2}}{\overline{\lambda^2}} \tag{3.8}$$

in which ν is the kinematic viscosity of fluid.

The definition of Kolmogorov's local scale l is given by[16]

$$l = (\nu^3/\epsilon)^{1/4} \tag{3.9}$$

A transformation of the Eulerian description in turbulence characteristics to the Lagrangian one can be made by use of the experimental relation of Hay and Pasquill,[31] which is

$$\frac{T_L}{T_E} \sim \left(\frac{u'}{U}\right)^{-1} \tag{3.10}$$

in which T_E and T_L are the Eulerian and the Lagrangian integral time-scales.

Table 3-1 Some turbulence characteristics in forms of universal function.

Turbulence Properties	Case A	Case B	Case C
Turbulence Intensity	$\frac{u'}{U_f(U/U_f)^{1/3}}=\phi_{u'}{}^a\left(\frac{z}{H}\right)$	$\frac{u'}{U_f}=\phi_{u'}{}^b\left(\frac{z}{H}\right)$	$\frac{u'}{U_f}=\phi_{u'}{}^c\left(\frac{z}{H}\right)$
Eulerian Mean Scale	$\frac{L_E}{H(U/U_f)}=\phi_{LE}{}^a\left(\frac{z}{H}\right)$	$\frac{L_E}{H}=\phi_{LE}{}^b\left(\frac{z}{H}\right)$	$\frac{L_E}{H(U/U_f)}=\phi_{LE}{}^c\left(\frac{z}{H}\right)$
Energy Dissipation Rate	$\frac{\epsilon}{U_f{}^3/H}=\phi_\epsilon{}^a\left(\frac{z}{H}\right)$	$\frac{\epsilon}{U_f{}^3/H}=\phi_\epsilon{}^b\left(\frac{z}{H}\right)$	$\frac{\epsilon}{U_f{}^3/H(U/U_f)}=\phi_\epsilon{}^c\left(\frac{z}{H}\right)$
Taylor's Dissipation Scale	$\frac{\lambda}{H(U_fH/\nu)^{-1/2}(U/U_f)^{1/2}}=\phi_\lambda{}^a\left(\frac{z}{H}\right)$	$\frac{\lambda}{H(U_fH/\nu)^{-1/2}}=\phi_\lambda{}^b\left(\frac{z}{H}\right)$	$\frac{\lambda}{H(U_fH/\nu)^{-1/2}(U/U_f)^{1/2}}=\phi_\lambda{}^c\left(\frac{z}{H}\right)$
Kolmogorov's Local Scale	$\frac{l}{H(U_fH/\nu)^{-3/4}}=\phi_l{}^a\left(\frac{z}{H}\right)$	$\frac{l}{H(U_fH/\nu)^{-3/4}}=\phi_l{}^b\left(\frac{z}{H}\right)$	$\frac{l}{H(U_fH/\nu)^{-3/4}(U/U_f)^{1/4}}=\phi_l{}^c\left(\frac{z}{H}\right)$
Relation between Lagrangian and Eulerian System	$T_L=\frac{L_L}{U}\sim\frac{U}{u'}T_E=\frac{L_E}{u'}$		
Lagrangian Mean Scale	$\frac{L_L}{H(U/U_f)^{5/3}}=\phi_{LL}{}^a\left(\frac{z}{H}\right)$	$\frac{L_L}{H(U/U_f)}=\phi_{LL}{}^b\left(\frac{z}{H}\right)$	$\frac{L_L}{H(U/U_f)^2}=\phi_{LL}{}^c\left(\frac{z}{H}\right)$
Diffusion Coefficient	$\frac{D}{U_fH(U/U_f)^{4/3}}=\phi_D{}^a\left(\frac{z}{H}\right)$	$\frac{D}{U_fH}=\phi_D{}^b\left(\frac{z}{H}\right)$	$\frac{D}{U_fH(U/U_f)}=\phi_D{}^c\left(\frac{z}{H}\right)$

Eq. (3.10) can be also derived by the similarity theory of Kolmogorov, as already described in 2.1.

Under the assumption of frozen turbulence of Taylor, the Lagrangian integral time-scale T_L and the turbulent diffusion coefficient D will be then expressed as

$$T_L\sim\frac{L}{u'} \tag{3.11}$$

$$D=\overline{u^2}T_L\sim u'L\sim\epsilon^{-1/3}L^{4/3} \tag{3.12}$$

In Table 3-1, **Case A** is obtained from Eqs. (3.4), (3.6) and (3.7), the resultant expression for the turbulence intensisty is

$$\frac{u'}{U_f(U/U_f)^{1/3}}=\phi_{u'}\left(\frac{z}{H}\right) \tag{3.13}$$

Comparing this to Eq.(3.3) which shows the dependence of the turbulence intensity on the friction velocity alone, the turbulence intensity given by Eq. (3.13) depends not only on the friction velocity but also on the ratio of the local mean velocity to the friction velocity.

Based on the Eqs.(3.3), (3.6) and (3.7), **Case B** will be obtained, in which the

Eulerian integral scale is given by

$$\frac{L}{H}=F_L\left(\frac{z}{H}\right) \tag{3.14}$$

Eq.(3.14) corresponds with the expression obtained by Velikanov,[32] under the assumption of constant Strouhal number.

3.3 Specific Forms of Universal Function

The expression of Eq. (3.6) may be considered to be more reliable than Eqs. (3.3) and (3.4), which are deduced through dimensional considerations and not deterministic. In the following, **Case C** will be then omitted.

Case A : The specific form of universal function for the Eulerian integral scale will be obtained from the following model of a turbulence field. The Eulerian integral time-scale depends mainly on the turbulence structure of low frequency range, which is controlled by the property of a intermittent upward flow in a free surface shear flow. Therefore, it will depend mainly on the period of the intermittent upward flow which is generated near the channel bed. Considering that the quantity, which has the dimension of time and is made from the representative parameters of geometrical and bounday conditions, will be H/U_f, then the Eulerian integral time-scale can be represented by the function of H/U_f alone, independent of the vertical position from the channel bed. Finally, under the assumption of frozen turbulence, the Eulerian integral scale L will be given by

$$\frac{L}{H(U/U_f)}\sim\text{const.} \tag{3.15}$$

in which the constant is universal. This expression corresponds to the experimental relation by Engelund.[30]

The first approximation for the energy dissipation rate is replaced by the energy production rate, which is expressed on the basis of a linear distribution of turbulent shear stress and of a logarithmic distribution of local mean velocity. However, comparing the Laufer's experimental results,[33),34)] this approximation is too small near the free surface, so it is modified to

$$\frac{\epsilon}{U_f^3/H}\sim\left(\frac{z}{H}\right)^{-1} \tag{3.16}$$

From the combination of Eqs. (3.6), (3.15) and (3.16), the turbulence intensity becomes

$$\frac{u'}{U_f(U/U_f)^{1/3}}\sim\left(\frac{z}{H}\right)^{-1/3} \tag{3.17}$$

Case B : Many specific forms of universal function for the turbulence intensity and the Eulerian integral scale have been proposed experimentally. Some of them are as follows :

For the turbulence intensity, Jonsson[5] has expressed the following relation from the interpolation of experimental results, that is

$$\frac{u'}{U_f}=2.0-1.3\left(\frac{z}{H}\right)\qquad\text{for}\quad 0.1\leq\frac{z}{H}\leq 1.0 \tag{3.18}$$

Velikanov[32] assumed that the Strouhal number, which consists of the reciprocal value of Eulerian integral time-scale, depth and local mean velocity, that is

$$S_h = \frac{H}{UT_E} \tag{3.19}$$

is constant for a free surface shear flow, and that it is equal to 0.73 throughout a vertical section. Hence, under the assumption of frozen turbulence, the Eulerian integral scale becomes

$$\frac{L}{H} = 1.4 \tag{3.20}$$

This relation means that the macro-structure of turbulence is characterized by the eddy which has a constant length in the longitudinal direction, in contrast with Eq. (3.15) where that is characterized by the intermittent upward flow with a constant period.

From the combination of Eqs.(3.6), (3.18) and (3.20), the energy dissipation rate becomes

$$\frac{\epsilon}{U_*^3/H} \sim \left\{2.0 - 1.3\left(\frac{z}{H}\right)\right\}^3 \tag{3.21}$$

The verification of these specific forms described above should be examined experimentally.

4. Statistical Effects of Finite Evaluating Time

4.1 Running and Sampling Time

Because of an imperfect response of measuring apparatus and a restricted duration of measurement, an estimator of a turbulence characteristics is sometimes distorted from the actual one. For instance, a measured instantaneous value should be regarded to be averaged over some running time for the real instantaneous value. Furthermore, since an estimator of mean quantity is obtained from averaging over some finite sampling time for the measured instantaneous value, it is not always corresponding to the real mean quantity, which is defined with an infinitesimally short running time and an infinitely long sampling time.

When the sampling for an instantaneous value measured with running time s is continued during the period from $(t_0 - T/2)$ to $(t_0 + T/2)$, the estimator of mean quantity, $\langle M\rangle_{T(t_0),s}$, is evaluated statistically by its lower-order moments[35], that is, bias $B[M]$, variance $VAR[M]$, and mean sqare error $MSE[M]$, which are defined as

$$B[M] = E[\langle M\rangle_{T(t_0),s}] - M = \langle M\rangle_{T,s} - M \tag{4.1}$$

$$VAR[M] = E[(\langle M\rangle_{T(t_0),s} - \langle M\rangle_{T,s})^2] \tag{4.2}$$

$$MSE[M] = E[(\langle M\rangle_{T(t_0),s} - M)^2] = VAR[M] + B^2[M] \tag{4.3}$$

in which the symbol E means the expected value of the quantity in parenthesis, M is the real mean value, $\langle M\rangle_{T,s}$ is the expected value of $\langle M\rangle_{T(t_0),s}$.

4.2 Evaluation of Estimated Turbulence Parameter

Mean Velocity : A measured instantaneous velocity $u_s(t)$ is expressed as

$$u_s(t)=\frac{1}{s}\int_{t-s/2}^{t+s/2}u(t)dt \tag{4.4}$$

in which $u(t)$ is the exact instantaneous velocity, s is the running time. And the estimated mean velocity $\langle U\rangle_{T(t_0),s}$ is given by

$$\langle U\rangle_{T(t_0),s}=\frac{1}{T}\int_{t_0-T/2}^{t_0+T/2}u_s(t)dt \tag{4.5}$$

Then, the expected value of estimated mean velocity, $\langle U\rangle_{T,s}$, becomes

$$\langle U\rangle_{T,s}=\lim_{T_0\to\infty}\frac{1}{T_0}\int_{-T_0/2}^{T_0/2}\langle U\rangle_{T(t_0),s}\,dt_0=\lim_{T_0\to\infty}\frac{1}{T_0}\int_{-T_0/2}^{T_0/2}u(t)dt=U \tag{4.6}$$

in which U is the real mean velocity. Eq. (4.6) means that there exists no bias in a mean velocity measurement.

The variance or the mean square error of the estimator of mean velocity can be deduced from Eqs. (4.2) or (4.3) to be

$$\begin{aligned}VAR\,[U]=MSE\,[U]&=\lim_{T_0\to\infty}\frac{1}{T_0}\int_{-T_0/2}^{T_0/2}(\langle U\rangle_{T(t_0),s}-U)^2dt_0\\&=\lim_{T_0\to\infty}\frac{1}{T_0}\int_{-T_0/2}^{T_0/2}\left\{\frac{1}{T}\int_{t_0-T/2}^{t_0+T/2}(u_s(t)-U)dt\right\}^2dt_0\\&=\frac{2}{T^2}\int_0^T(T-\tau)\,\overline{u_s'(t)u_s'(t+\tau)}\,d\tau\end{aligned} \tag{4.7}$$

in which

$$u_s'(t)=u_s(t)-U \tag{4.8}$$

$$u_s'(t)u_s'(t+\tau)=\lim_{T_0\to\infty}\frac{1}{T_0}\int_{-T_0/2}^{T_0/2}u_s'(t)u_s'(t+\tau)dt \tag{4.9}$$

Noticing that in this section u' does not mean the root mean square of u but an instantaneous fluctuating velocity.

From the property of covariance function $\overline{u_s'(t)u_s'(t+\tau)}$, which will be seen later, it will be concluded that $VAR[U]$ or $MSE[U]$ decreases with increasing of s or T. An example of statistical effects of running and sampling time for the estimator of mean velocity is presented in Fig. 4-1, which shows that the longer running and sampling time will produce the better estimator of mean velocity. Therefore, since the selection of a long sampling time is not so difficult, it will be desirable in a measurement of mean velocity to use an apparatus of long running time, that is, an equipment which has large inertia.

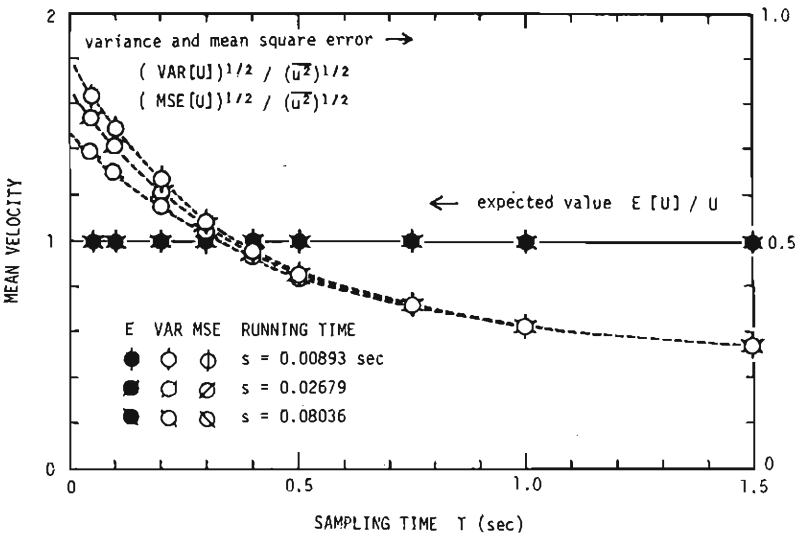

Fig. 4-1 An example of statistical effects of evaluating time in the estimation of mean velocity.

Turbulent Velocity : An apparent turbulent velocity is defined as the difference of $u_s(t)$ and $\langle U\rangle_{T(t_0),s}$, and hence the estimator of squared turbulent velocity, $\langle\overline{u'^2}\rangle_{T(t_0),s}$ is expressed as

$$\langle\overline{u'^2}\rangle_{T(t_0),s}=\frac{1}{T}\int_{t_0-T/2}^{t_0+T/2}(u_s(t)-\langle U\rangle_{T(t_0),s})^2\,dt \tag{4.10}$$

Then, the expected value of $\langle\overline{u'^2}\rangle_{T,s}$ is to be

$$\langle\overline{u'^2}\rangle_{T,s}=\langle\overline{u'^2}\rangle_{\infty,s}-\frac{2}{T^2}\int_0^T(T-\tau)\overline{u_s'(t)u_s'(t+\tau)}\,d\tau \tag{4.11}$$

This relation means that $\langle\overline{u'^2}\rangle_{T,s}$ increases with increasing samling time and with decreasing running time.

The variance and the mean square error of squared turbulent velocity are given by

$$VAR[\overline{u'^2}]=E[(\langle\overline{u'^2}\rangle_{T(t_0),s})^2]-(\langle u'^2\rangle_{T,s})^2 \tag{4.12}$$

$$MSE[\overline{u'^2}]=E[(\langle\overline{u'^2}\rangle_{T(t_0),s})^2]-2\langle u'^2\rangle_{T,s}\overline{u'^2}+(\overline{u'^2})^2 \tag{4.13}$$

In these equations, $E[(\langle\overline{u'^2}\rangle_{T(t_0),s})^2]$ and $\langle\overline{u'^2}\rangle_{T,s}$ is nearly zero for small T and $E[(\langle\overline{u'^2}\rangle_{T(t_0),s})^2]$ approaches to $(\langle\overline{u'^2}\rangle_{T,s})^2$ for large T. From these properties, the following conclusions will result, that is, $VAR[\overline{u'^2}]$ is very small when T is either very small or very large, and shows the maximum at a certain critical value of T which depends on s. On the other hand, $MSE[\overline{u'^2}]$ decreases uniformly with increasing T, and may be approximated to $(\overline{u'^2})^2$ at small T and to $(\overline{u'^2}-\langle\overline{u'^2}\rangle_{T,s})^2$ at large T. These properties are presented in Fig. 4-2.

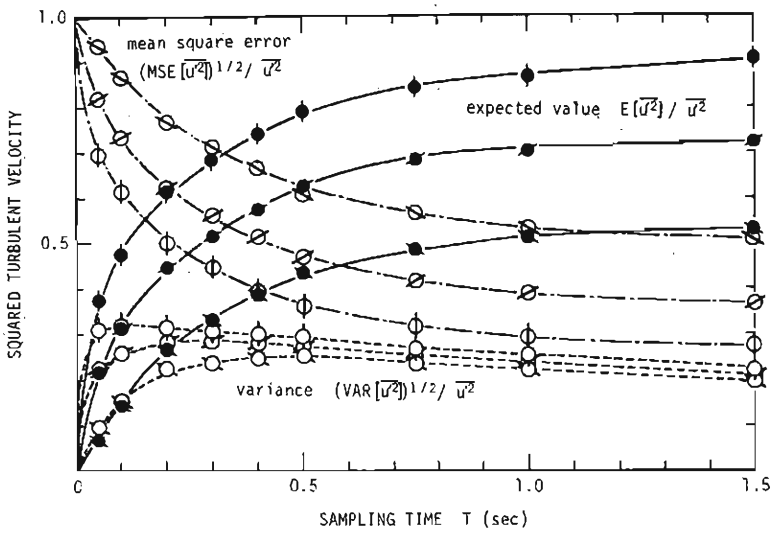

Fig. 4-2 An example of statistical effects of evaluating time in the estimation of turbulent velocity.

Through the above consideration, it will be concluded that the shorter running time and the longer sampling time will produce the better estimator of squared turbulent velocity. Therefore, it will be desirable in a measurement of turbulent velocity to use an apparatus of high sensitivity, contrasted to a measurement of mean velocity.

Covariance Function: Using the definition of an unbiased covariance function, the sample auto-covariance function of $u(t)$, $\langle R(\tau)\rangle_{T(t_0),s}$, becomes to be

$$\langle R(\tau)\rangle_{T(t_0),s}=\frac{1}{T-\tau}\int_{t_0-T/2}^{t_0+T/2-\tau}(u_s(t)-\langle U\rangle_{T(t_0),s})(u_s(t+\tau)-\langle U\rangle_{T(t_0),s})dt$$

$$=\frac{1}{T-\tau}\left\{\int_{t_0-T/2}^{t_0+T/2-\tau}u_s'(t)u_s'(t+\tau)dt\right.$$

$$\left.-\langle U'\rangle_{T(t_0),s}\int_{t_0-T/2+\tau}^{t_0+T/2-\tau}u_s'(t)dt-\tau(\langle U'\rangle_{T(t_0),s})^2\right\}\quad\text{for } 0\leq\tau<T \qquad (4.14)$$

in which

$$\langle U'\rangle_{T(t_0),s}=\langle U\rangle_{T(t_0),s}-U \qquad (4.15)$$

The expected sample covariance function, $\langle R(\tau)\rangle_{T,s}$, will be obtained after some calculations as

$$\langle R(\tau)\rangle_{T,s}=\langle R(\tau)\rangle_{\infty,s}-\frac{2}{T(T-\tau)}\left\{\frac{\tau}{T}\int_0^T(T-\tau_1)\langle R(\tau_1)\rangle_{\infty,s}d\tau_1\right.$$

$$\left.+\int_0^{T-\tau}(T-\tau-\tau_1)\langle R(\tau_1)\rangle_{\infty,s}d\tau_1-\int_0^{\tau}(\tau-\tau_1)\langle R(\tau_1)\rangle_{\infty,s}d\tau_1\right\} \qquad (4.16)$$

in which

$$\langle R(\tau)\rangle_{\infty,s}=\overline{u_i'(t)u_i'(t+\tau)}=\frac{1}{s^2}\left\{\int_{\tau-s}^{\tau}(\tau_1-\tau+s)R(\tau_1)d\tau_1\right.$$
$$\left.+\int_{\tau}^{\tau+s}(-\tau_1+\tau+s)R(\tau_1)d\tau_1\right\} \tag{4.17}$$

The second term of right hand side in Eq. (4.16) may be negligible for large T, and $\langle R(\tau)\rangle_{\infty,s}$ may be approximated to $R(\tau)$ for small s, and hence a sample covariance function will approach to the real one when the running time is sufficiently small and the sampling time sufficiently large.

Integrating $\langle R(\tau)\rangle_{\infty,s}$ with τ from zero to infinity, the following relation will be obtained from Eq. (4.17).

$$\int_0^{\infty}\langle R(\tau)\rangle_{\infty,s}d\tau=\int_0^{\infty}R(\tau)d\tau \qquad i.e. \quad \langle\overline{u'^2}\rangle_{\infty,s}\langle T_m\rangle_{\infty,s}=\overline{u'^2}T_m \tag{4.18}$$

which shows that the product of squared turbulent velocity $\overline{u'^2}$ and integral time-scale T_m is independent of running time under the condition of a sufffciently large sampling time.

For example, let the covariance function be expressed by an exponential functional form, that is,

$$R(\tau)=\overline{u'^2}\exp\left(-\frac{\tau}{T_m}\right) \tag{4.20}$$

then, $\langle R(\tau)\rangle_{\infty,s}$ will become approximately to

$$\langle R(\tau)\rangle_{\infty,s}=\langle\overline{u'^2}\rangle_{\infty,s}\exp\left(-\frac{\tau}{\langle T_m\rangle_{\infty,s}}\right) \tag{4.21}$$

Strictly speaking, Eq. (4.21) does not coincide with the result of Eq. (4.17) especially in small τ, but may be adopted as an approximate relation based on Eq. (4.18).

Substituting Eq. (4.21) into Eq. (4.16), the expected sample covariance function will be given by

$$\frac{\langle R(\tau)\rangle_{T,s}}{\langle\overline{u'^2}\rangle_{\infty,s}}=e^{-\tau/\langle T_m\rangle_{\infty,s}}-\frac{2(\langle T_m\rangle_{\infty,s})^2}{T(T-\tau)}\left\{\left(\frac{T-\tau}{\langle T_m\rangle_{\infty,s}}+e^{-(T-\tau)/\langle T_m\rangle_{\infty,s}}-1\right)\right.$$
$$\left.-\left(\frac{\tau}{\langle T_m\rangle_{\infty,s}}+e^{-\tau/T\langle m\rangle_{\infty,s}}-1\right)+\frac{\tau}{T}\left(\frac{T}{\langle T_m\rangle_{\infty,s}}+e^{-T/\langle T_m\rangle_{\infty,s}}-1\right)\right\} \tag{4.22}$$

The combination of Eqs. (4.7) and (4.21) results in the following relation, that is,

$$VAR[U]=MSE[U]=2\langle\overline{u'^2}\rangle_{\infty,s}\frac{T/\langle T_m\rangle_{\infty,s}+e^{-T/\langle T_m\rangle_{\infty,s}}-1}{(T/\langle T_m\rangle_{\infty,s})^2} \tag{4.23}$$

Putting $\tau=0$ in Eq. (4.17) and substituting Eq. (4.20) into the resultant equation, it follows that

$$\frac{\langle\overline{u'^2}\rangle_{\infty,s}}{\overline{u'^2}}=\frac{T_m}{\langle T_m\rangle_{\infty,s}}=2\,\frac{s/T_m+e^{-s/T_m}-1}{(s/T_m)^2} \tag{4.24}$$

It may be concluded from above considerations that the effect of finite sampling time in a measurement of covariance function is significant over any lag time, as seen in Fig. 4–3.

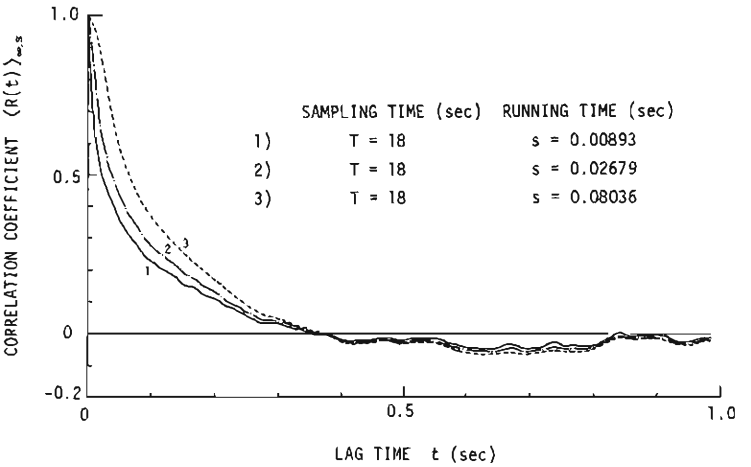

Fig. 4-3 (a) An example of statistical effects of running time in the estimation of correlatior coefficient.

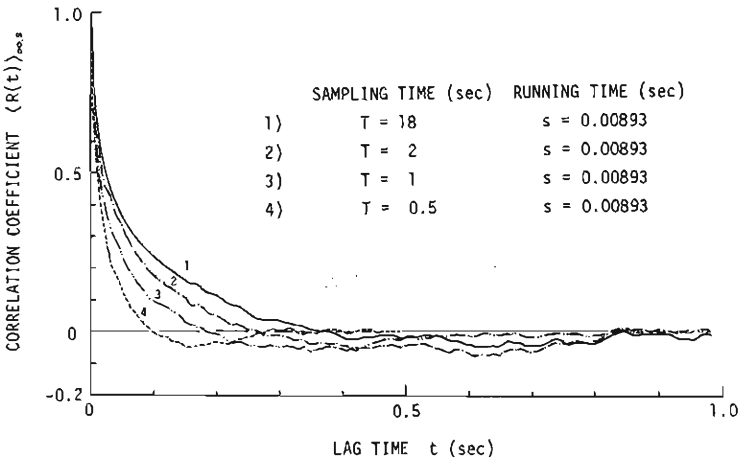

Fig. 4-3 (b) An example of statistical effects of sampling time in the estimation of correlation coefficient.

Spectrum Function: The spectrum function is defined by the Fourier transform of the covariance function, then the sample spectrum function $\langle S(f)\rangle_{T(t_0),s}$ is

$$\langle S(f)\rangle_{T(t_0),s} = 4\int_0^T \langle R(\tau)\rangle_{T(t_0),s} \cos 2\pi f\tau \, d\tau \tag{4.25}$$

and also the expected sample spectrum function is

$$\langle S(f)\rangle_{T,s} = 4\int_0^T \langle R(\tau)\rangle_{T,s} \cos 2\pi f\tau \, d\tau \tag{4.26}$$

When the sampling time is infinite, the sample covariance function may be re-written by the inverse Fourier trnsform of the sample spectrum function,

$$\langle R(\tau)\rangle_{\infty,s} = \int_0^\infty \langle S(f)\rangle_{\infty,s} \cos 2\pi f\tau \, df \tag{4.27}$$

Substituting Eq. (4.27) into Eq. (4.11),

$$\langle \overline{u'^2}\rangle_{T,s} = \langle \overline{u'^2}\rangle_{\infty,s} - \frac{2}{T^2}\int_0^T (T-\tau)\int_0^\infty \langle S(f)\rangle_{\infty,s} \cos 2\pi f\tau \, df d\tau \tag{4.28}$$

Noticing the fact that the sample spectrum shows how the average power of $u'_s(t)$ is distributed over frequencies, this relation is rewritten by

$$\begin{aligned}\int_0^\infty \langle S(f)\rangle_{T,s}\, df &= \int_0^\infty \langle S(f)\rangle_{\infty,s}\, df - \frac{2}{T^2}\int_0^T (T-\tau)\int_0^\infty \langle S(f)\rangle_{\infty,s} \cos 2\pi f\tau \, df d\tau \\ &= \int_0^\infty \left(1 - \frac{\sin^2 \pi fT}{(\pi fT)^2}\right)\langle S(f)\rangle_{\infty,s}\, df \end{aligned} \tag{4.29}$$

Putting $\tau = 0$ in Eq. (4.17),

$$\langle \overline{u'^2}\rangle_{\infty,s} = \frac{2}{s^2}\int_0^s (s-\tau) R(\tau) d\tau \tag{4.30}$$

which is rewritten by

$$\int_0^\infty \langle S(f)\rangle_{\infty,s}\, df = \int_0^\infty \frac{\sin^2 \pi fs}{(\pi fs)^2} S(f) df \tag{4.31}$$

From the combination of Eqs. (4.29) and (4.31), the resultant expression will be

$$\langle S(f)\rangle_{T,s} = \frac{\sin^2 \pi fs}{(\pi fs)^2}\left(1 - \frac{\sin^2 \pi fT}{(\pi fT)^2}\right) S(f) \tag{4.32}$$

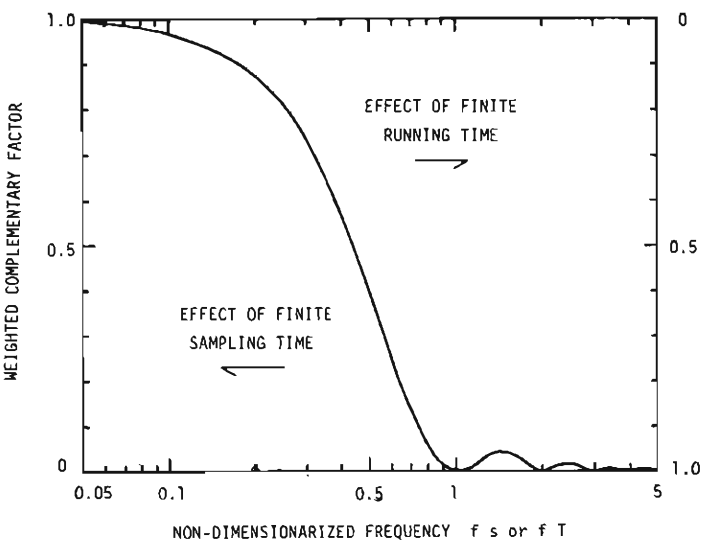

Fig. 4-4 A sample of weighted complementary factor.

Smith[36] has obtained a similar result to Eq. (4.32) with a somewhat different method.

Eq. (4.32) shows that the sample spectrum is weighted by a complementary factor $\frac{\sin^2 \pi fs}{(\pi fs)^2}\left(1-\frac{\sin^2 \pi fT}{(\pi fT)^2}\right)$ to the exact spectrum. The effect of running time modifies the spectrum at high frequency range, while that of sampling time at low frequency range. A sample of weighted complementary factor is illustrated in Fig.4–4.

5. Experimental Investigation of Turbulence Characteristics

5.1 Experimental Arrangement and Data Processing

To investigate the Eulerian turbulence characteristics in a free surface shear flow, two series of turbulence measurement were carried out. One consisted of laboratory experiments in a smooth-walled rectangular channel of 13 m in length and 0.40 m in width. The other was field observations made at the Nobi Agricultural Canal which is located along the left-hand side levee of the River Kiso. This canal is a concrete-coated rectangular channel of 600 m in length and 18 m in width, and the channel bed is set up at 1/480 in slope.

Hot-film probes of quartz-coated wedge-shaped (DISA 55A8l) and of quartz-coated V-array (DISA 55A89), both 1 mm in length and 0.35 mm in width, were used to measure the longitudinal and the vertical components of turbulent velocity in the laboratory channel, and an amplifier (DISA 55A10) was used to operate the probes at a constant temperature with an overheating ratio of 0.05. The hot-film output was linearized using a linearizer (DISA 55D10). The usage of the hot-film anemometer requires sufficiently clean water to avoid an attachment of inpurity on the probe. On the other hand, a propeller-dynamo current meter (TOHO-DENTAN CM-1B) of 12.8 cm in diameter was used in field observations. Since a time-constant of this current meter is about 0.5 sec, it is not suitable for a small-scale turbulence measurement, but may be useful for a large-scale turbulence measurement.

The velocity signal was FM tape recorded using a data recorder (TEAC R-400), and the analogue recorded signal was then digitalized by A-D converter (TEAC DP-300) through low-pass prefiltering to cut off a high frequency noise involved in the signal. The digitally sampled data were processed by means of Blackman and Tukey, using a digital computer (KDC-Ⅱ), locates in the main campus of Kyoto University.

The Lagrangian turbulence measurements were performed by instantaneous tracking of floating particle-tracers on the free surface in two laboratory channels, one of which is a smooth-walled rectangular channel of 10 m in length and 0.25 m in width, and the other 15 m in length and 0.50 m in width, is smooth side-walled and of rough bed coated by sand grains. The dimension of solid-paraffin particle (specific weight 0.873) which were used as tracers is 3 mm in diameter and 2 mm in thickness. The tracking of floating particles was made by means of photographical technique with strobo-flash lighting, and 200 observations of tracking were repeated for each test run. The Lagrangian data were processed in a similar manner to the Eulerian ones.

The discharge and the depth of flow were artificially controlled in all the test runs. The width-depth ratio B/H was always kept larger than 10 to satisfy the condition of two-dimensionality of flow in the central parts of the channel. Hydraulic conditions of the Eulerian and the Lagrangian expeiments are listed in Table 5-1. In this paper, the experimental results obtained by other investigators were also used for the verification

of the turbulence characteristics, and the hydraulic conditions of their experiments are listed in Table 5-2.

Table 5-1 Hydraulic conditions of Eulerian turbulence measurements.

Case	width B(cm)	depth H(cm)	aspect ratio B/H	mean velocity U_m(cm/sec)	friction velocity U_f(cm/sec)	velocity ratio U_m/U_f	Reynolds number $R_e=U_mH/\nu$	Froude number $F_r=U_m/\sqrt{gH}$
SM-1	50	8.00	6.3	69.0	4.00	17.3	4.34×10^4	0.779
SM-2	50	5.02	10.0	43.0	2.30	18.7	1.70×10^4	0.613
SM-3	50	3.24	15.4	34.4	2.55	13.5	8.82×10^3	0.610
SM-4	50	2.38	21.0	21.9	1.13	19.4	4.10×10^3	0.453
SS-1	50	6.78	7.4	141.8	8.11	17.5	7.59×10^4	1.74
SS-2	50	5.00	10.0	140.5	7.72	18.2	5.20×10^4	1.86
SS-3	50	2.58	19.4	103.4	5.00	20.7	2.12×10^4	2.06
SS-4	50	2.44	20.5	100.8	4.80	21.0	1.95×10^4	2.06
RM-1	50	3.10	16.1	54.5	3.81	14.3	1.20×10^4	0.989
RS-1	50	2.09	23.9	47.9	3.13	15.3	7.11×10^3	1.06
I-1	1800	158	11.4	109.7	5.77	19.0	1.52×10^6	0.279
I-2	1800	92	19.6	137.6	7.65	18.0	1.10×10^6	0.458
I-3	1800	49	36.7	81.4	3.94	20.7	6.50×10^5	0.371

Table 5-2 Hydraulic conditions of Lagrangian turbulence measurements.

Case	width B(cm)	depth H(cm)	aspect ratio B/H	mean velocity U_m(cm/sec)	friction velocity U_f(cm/sec)	velocity ratio U_m/U_f	Reynolds number $R_e=U_mH/\nu$	Froude number $F_r=U_m/\sqrt{gH}$
L-1	25	9.52	2.63	66.8	3.99	16.7	5.49×10^4	0.692
L-2	25	6.73	3.71	54.5	2.76	19.7	3.99×10^4	0.671
L-3	25	4.00	6.25	48.0	1.68	28.6	1.41×10^4	0.767

5.2 Probability Distribution of Velocity Fluctuation

In general, the probability distribution of velocity fluctuation in isotropic turbulence, $p(u)$, is represented by normal Gaussian distribution, that is

$$p(u)=\frac{1}{\sqrt{2\pi}\,u'}\exp\left(-\frac{u^2}{2\overline{u^2}}\right) \tag{5.1}$$

and the skewness factor S and the flatness factor F, which are defined as

$$S=\frac{\overline{u^3}}{(\overline{u^2})^{3/2}}\quad,\qquad F=\frac{\overline{u^4}}{(\overline{u^2})^{4/2}} \tag{5.2}$$

are to be 0 and 3, respectively. Similar results were obtained by Townsend,[37] Ippen & Raichlen,[41] and Hino[38] even in non-isotropic turbulence. However, the experimental results in boundary layer flow by Compte-Bellot[39] and Schraub & Klein,[40] and in

free surface shear flow by Rudis & Smutek[6] revealed that the probability distribution can not be expressed by Gaussian distribution and the skewness factor is varried with the distance from a boundary.

Examples of the probability distribution of longitudinal and vertical turbulent velocities are shown in Figs. 5-1 (a) and 5-1 (b), and the skewness factor in Fig. 5-2. The measurement of turbulent velocity were made by a dual-sensor hot-film probe

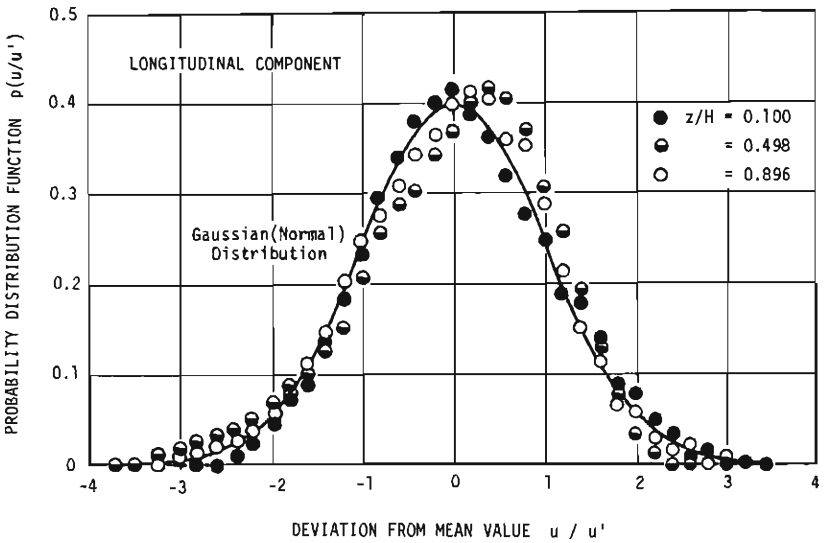

Fig. 5-1(a) An example of probability distribution of longitudinal turbulent velocity.

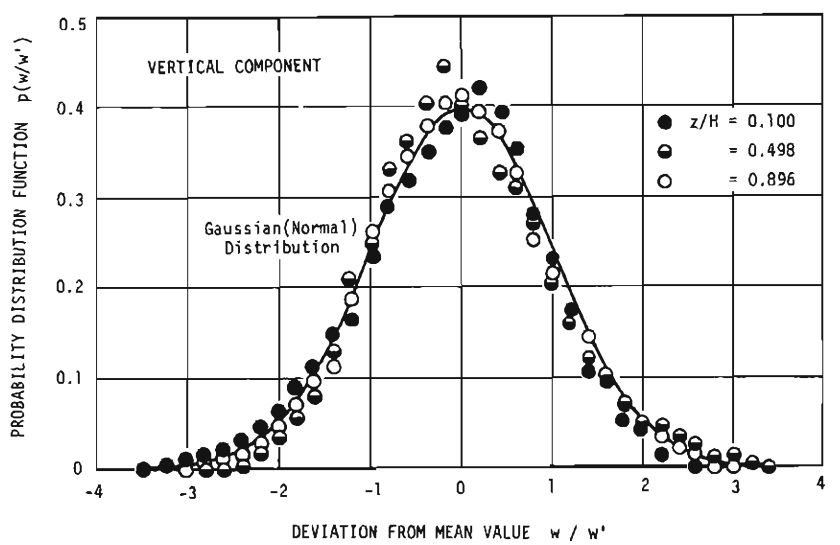

Fig. 5-1(b) An example of probability distribution of vertical turbulent velocity.

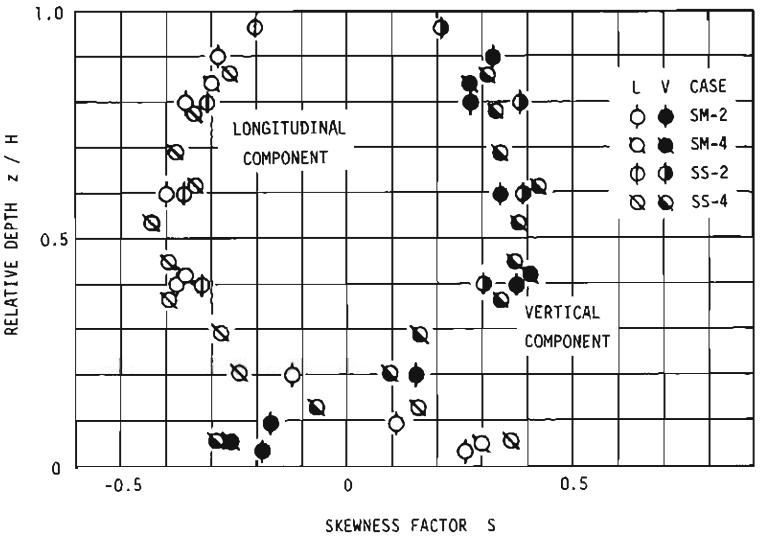

Fig. 5-2 Vertical distribution of skewness factor of longitudinal and vertical turbulent velocities.

(DISA 55A89), and the calculation was made using 5000 data digitalized with a sampling frequency 200 Hz. As it is seen in these figures, the probability distribution is approximately Gaussian at the transient region and at the region close to the free surface. The skewness factor of longitudinal component is positive near the channel bed, negative in central parts, and approaches zero near the free surface, while that of vertical component is negative near the channel bed, positive in central parts, and approaches zero near the free surface.

Such characteristics of probability distribution may be explained qualitatively as follows. That is, velocity fluctuations in a free surface shear flow are characterized by the mixing of fluid particle between upper and lower layers, and near the bottom an intermittent violent motion from upper layer is dominant ($u' > 0$, $w' < 0$), in central parts that from lower layer is dominant ($u' < 0$, $w' > 0$), and near the free surface the motion diminishes. The mechanics of the intermittent violent motion may be explained by the horse-shoe vortex theory.[41][42]

5.3 Correlation and Spectrum

Auto-Correlation Coefficient : Correlation techniques have been broadly used to investigate the turbulence characteristics because of the simplicity of calcution and the clearness of physical meaning. However, the correlation coefficient in a free surface shear flow becomes so complicated from the nature of multi-structural turbulence that it can not be expressed by a simple functional form. Furthermore, an estimated correlation coefficient is affected severely by the finiteness of sampling time. Therefore, the correlation coefficient is not always useful. It becomes effective under the suitable conditions of evaluating time, only when the turbulence is uni-structural or approximately uni-structural.

Fig. 5-3(a) shows an example of Eulerian auto-correlation coefficient in laboratory

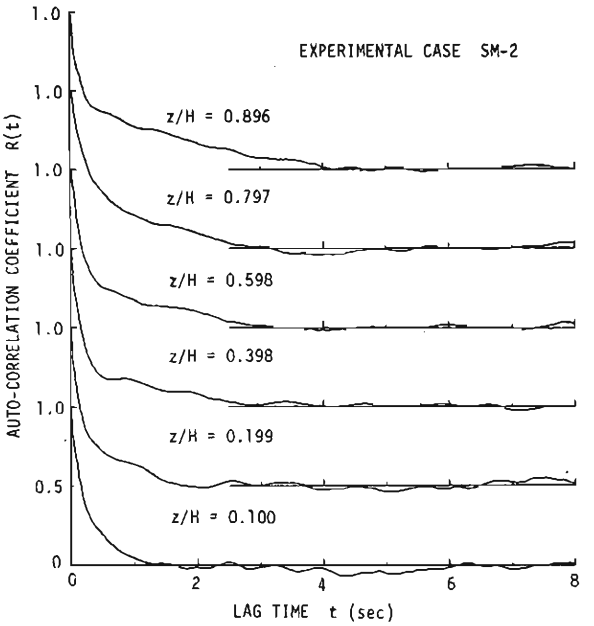

Fig. 5-3(a) An example of the Eulerian auto-correlation coefficient in laboratory experiments.

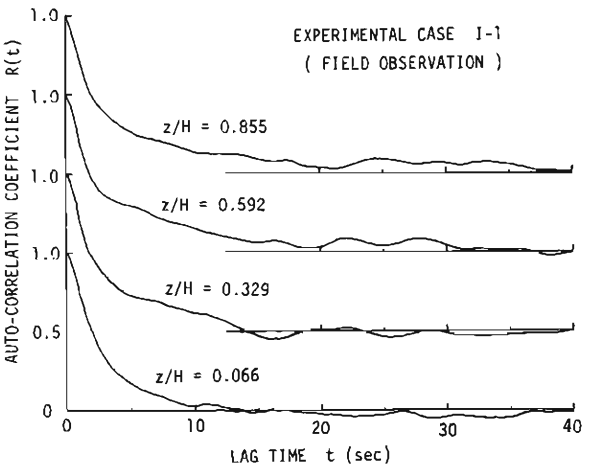

Fig. 5-3(b) An example of the Eulerian auto correlation coefficient in field observations.

experiments using the wedge-shaped hot-film probe (DISA 55A81) under the sampling frequency $f_s=200$ Hz, data amount $N=1000$, maximum lag $M=100$, number of repetitions $R=10$, and Fig. 5-3(b) in field observations using the propeller-dynamo current meter under $f_s=2$ Hz, $N=1000$, $M=100$, and $R=5$. As it is seen in these figures, in short lag time the auto-correlation coefficient of longitudinal

turbulent velocity decreases rapidly independent of vertical positions, and then approaches gradually to zero value. These characteristics may be explained by the nature of multi-structural turbulence. The effect of multi-structure is remarkable in the region near the free surface, and not so near the channel bed. This fact means that the

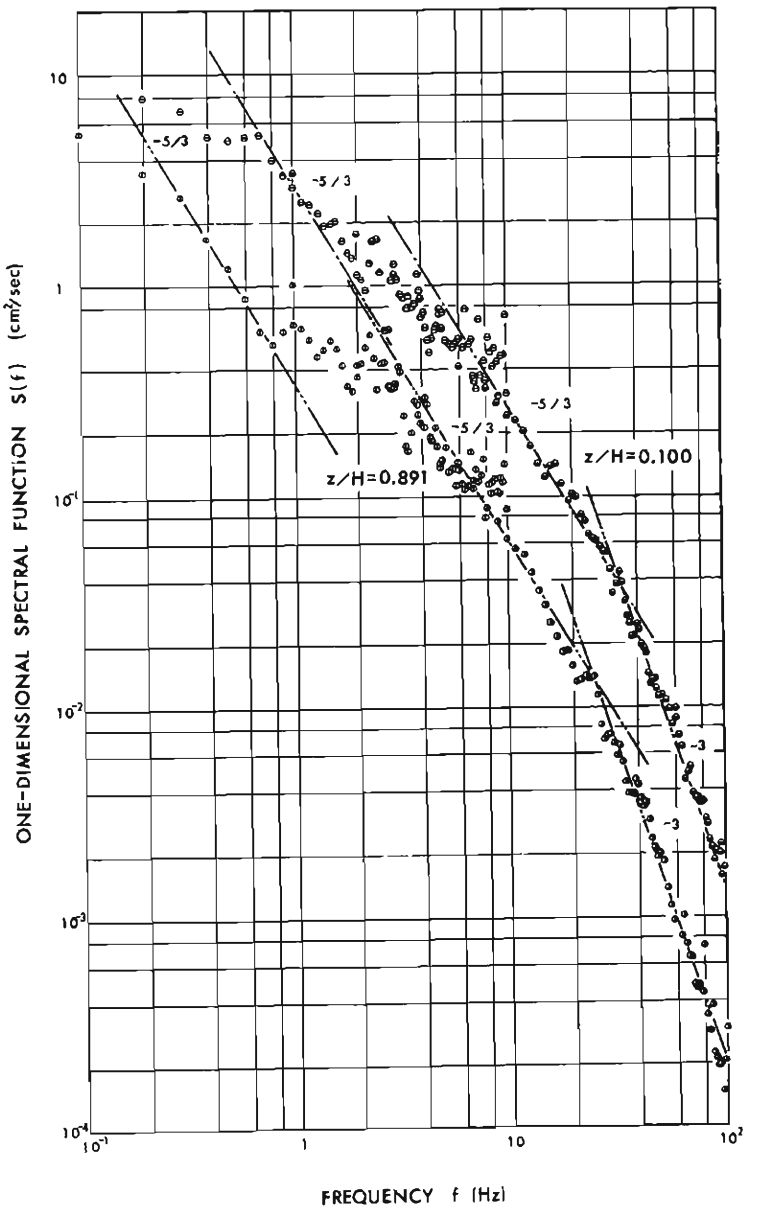

Fig. 5-4 An example of the Eulerian one-dimensional frequency spectrum of longitudinal turbulent velocity.

intermittent violent motion is dominant near the bed and the effect of multi-structure will be concealed. On the other hand, the intermittent violent motion generated near the bed is diminished during the upward transport, so that the nature of multi-structural turbulence will be remarkable near the free surface.

As already mentioned, it is difficult to express the auto-correlation coefficient in a whole lag time by a simple functional form, and the technique of "semi-scale" introduced by Panofsky,[43] which is based of the exponential functional form of auto-correlation coefficient, can not be applied to determine the integral scale. Therefore, the evaluation based on the spectrum should be used to determine the integral scale corresponding to a certain factor.

Frequency Power-Spectrum: An examples of the Eulerian one-dimensional frequency spectrum of longitudinal turbulent velocity is shown in Fig. 5-4, measured by a

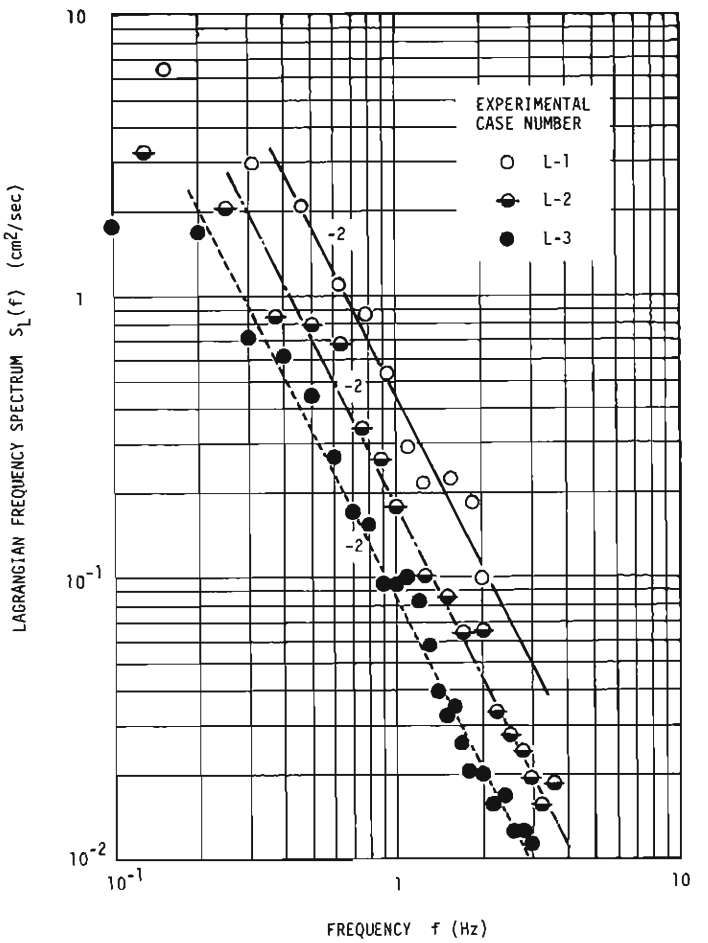

Fig. 5-5 An example of the Lagrangian one-dimensional frequency spectrum of longitudinal velocity on the free surface.

wedge-shaped hot-film probe (DISA 55A81). For convenience of calculation, two kinds of sampling frequency, $f_s=20$ Hz and 200 Hz, were used and the number of repetitions $R=2$ for the former and $R=10$ for the latter. The data amount are 1000 for both cases. Half-black circles in Fig. 5-4 represent the values estimated from the data of $f_s=200$ Hz.

These spectra are in good agreement with the Kolmogorov's -5/3 power law in both the regions of low and high frequencies. Similar results have been obtained by Yokosi[44] through field observations in the River Uji. The fact that -5/3 power law is established in more than two kinds of frequency ranges may be considered to be resulted from the nature of multi-structural turbulence. As seen in the Reynolds number similarity, a free surface shear flow in rectangular channel is essentially characterized by two geometrical parameters, the depth and the width, and hence a turbulence in a rectangular open channel has the nature of a double-structure. When the width is sufficiently large compared to the depth, the lower frequency range of the spectrum is characterized by the width, and the higher frequency range by the depth. Then, it may be concluded that the frequency range from 8 Hz to 20 Hz in Fig.5-4 is characterized by the depth. In higher frequency range than 20~30 Hz, both spectra seem to be represented by -3 power law. The verification of -3 power law in sufficiently high frequency ranges will require more precise experiments.

Fig.5-5 shows an example of the Lagrangian one-dimensional frequency spectrum of longitudinal turbulent velocity on the free surface. The measurements of the Lagrangian turbulent velocity were carried out by a tracking of floating particle tracers. The movement of each particle floating on the free surface was photographed at every 0.05 sec. Each test run was made by 100 observations of tracer tracking. As seen in Fig.5-5, the Lagrangian frequency spectrum in high frequency range is described by the -2 power law, which is coincident with the property in inertial sub-range presented by Eq.(2.12).

5.4 Turbulence Parameter

Among the various estimating methods for the turbulence parameters, the one using spectrum may be preferably applied for the turbulence in free surface shear flow, and others are affected with the nature of multi-structure and with the finiteness of evaluating time. Therefore, in this paper, turbulence parameters were estimated by the following procedure. When the measurement is performed under suitable conditions of evaluating time, the effect of multi-structure and finiteness of evaluating time are not so significant for the turbulence intensity. Then, the turbulence intensity is firstly determined from the root mean square of fluctuating velocity. Secondly, the energy dissipation rate is estimated from the spectrum property in inertial sub-range, in which the universal constant in Eq.(2.5) is assumed to be 0.48.[45] The Eulerian integral scale is determined lastly, using the previously estimated two parameters to Eqs. (2.10) and (2.21).

The estimations of turbulence intensity are illustrated in Figs.5-6(a) and 5-6(b), using a semi-log plot for the convenience of mutual comparison. The experimental results in free surface shear flows by Jonsson,[5] Raichlen[7], McQuivey & Richardson[8] and Engelund[30] are also given in these figures. In Fig.5-6(a), the turbulence intensity is normalized by the factor $U_f(U/U_f)^{1/8}$ corresponding to **Case A** in Table 3-1,

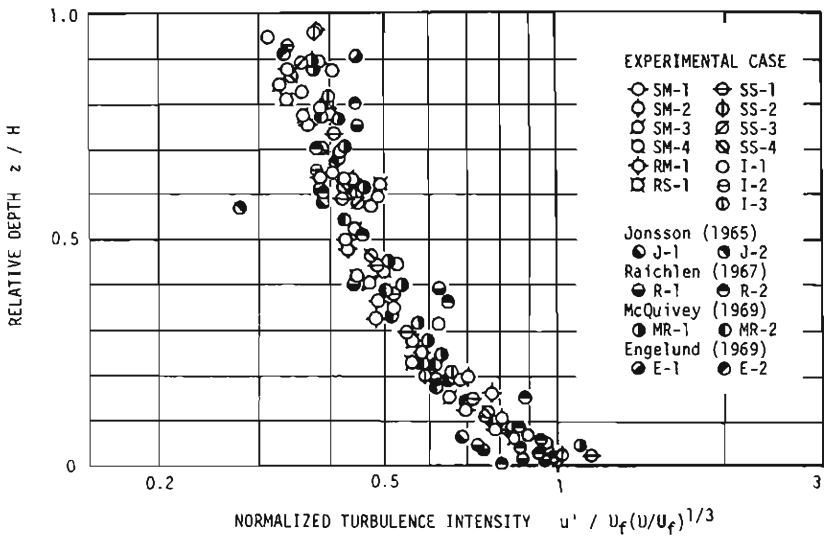

Fig. 5-6(a) Vertical distribution of the longitudinal turbulence intensity in a form of universal function corresponding to **Case A.**

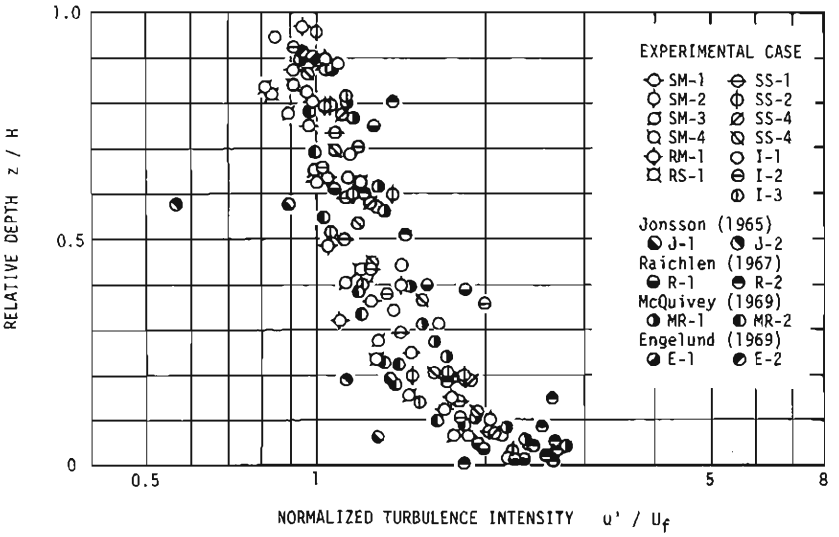

Fig. 5-6(b) Vertical distribution of the longitudinal turbulence intensity in a form of universal function corresponding to **Case B.**

and in Fig.5-6(b), by U_f alone corresponding to **Case B.** From the comparison of these figures, it will be concluded that the scattering of experimental values in Fig.5-6(a) is small compared to that in Fig.5-6(b). Therefore, the expression of Eq. (3.13) would be better than Eq.(3.3).

In Fig. 5-7 the turbulence intensity normalized by $U_f(U/U_f)^{1/3}$ is rearranged using a log-log plot, and the following interpolation form of the universal function will

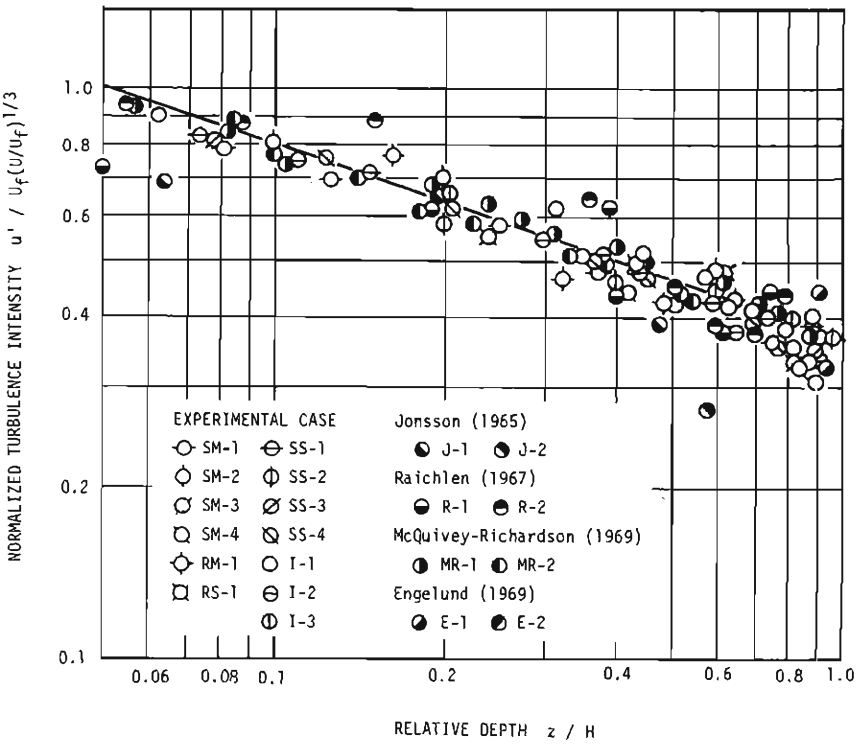

Fig. 5-7 Vertical distribution of the longitudinal turbulence intensity in a form of universal function corresponding to **Case A** (using a log-log plot).

result except near the channel bed, that is

$$\frac{(\overline{u'^2})^{1/2}}{U_f(U/U_f)^{1/3}} = 0.36\left(\frac{z}{H}\right)^{-1/3} \quad \text{for } 0.1 \leq z/H \leq 1.0 \tag{5.3}$$

Normalizing the estimated Eulerian integral scale in the forms of universal function corresponding to **Case A** and **B** in Table 3-1, Figs. 5-8(a) and 5-8(b) are presented. For comparison are also presented the experimental results by Ippen & Raichlen,[4] Jonsson[5] and Engelund,[30] which have been obtained from the integration of auto-correlation coefficient. An auto-correlation coefficient, however, depends severely on the finite sampling duraction, and sometimes is so complicated that can not be represented by simple functional form. Therefore, it may be considered that these experimental results are a few examples successfully estimated. The estimating method in this paper is unique and somewhat different from others, and the appropriateness of it should be discussed more precisely in future.

At first sight of Figs. 5-8(a) and 5-8(b), the scattering in the former seems to be smaller than that in the latter, so that the following interpolation formula corresponding to Eq. (3.15) will be obtained.

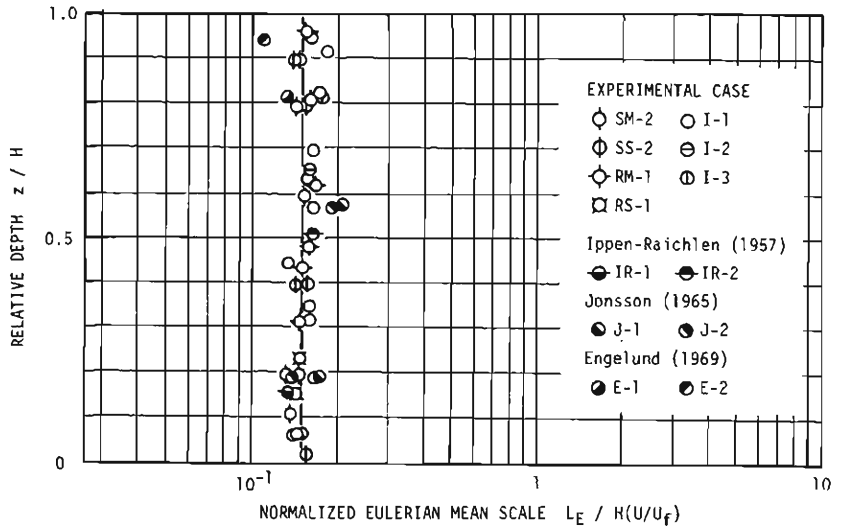

Fig. 5-8(a) Vertical distribution of the Eulerian integral scale of longitudinal turbulent velocity in a form of universal function corresponding to **Case A**.

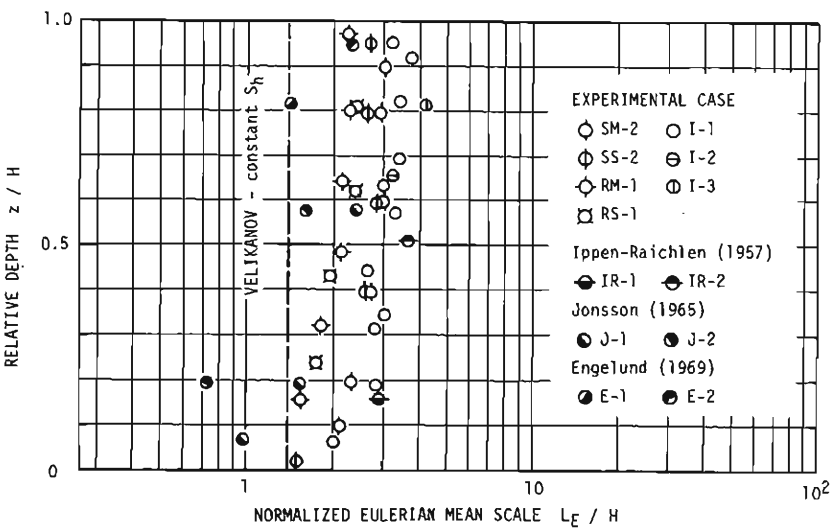

Fig. 5-8(b) Vertical distribution of the Eulerian integral scale of longitudinal turbulent velocity in a form of universal function corresponding to **Case B**.

$$\frac{L}{H(U/U_f^-)} = 0.15 \tag{5.4}$$

To examine the validity of the form of universal function for the energy dissipation rate proposed in **Case A** and **B** in Table 3-1, Fig. 5-9 was drawn up. While the

Table 5-3 Hydraulic conditions of Eulerian turbulence measurements referenced in this paper.

Investigator	Case	width B(cm)	depth H(cm)	aspect ratio B/H	mean velocity U_m(cm/sec)	friction velocity U_f(cm/sec)	velocity ratio U_m/U_f	Reynolds number $R_e=U_mH/\nu$	Froude number $F_r=U_m/\sqrt{gH}$
Ippen and Raichlen[1] (1957)	IR-1	121.9	3.23	37.7	180	8.05	22.4	5.20×10^4	3.20
	IR-2	121.9	2.77	44.0	220	9.77	22.5	5.43×10^4	4.22
Jonsson[2] (1965)	J-1	120	15.6	7.7	72	6.70	10.7	1.12×10^5	0.582
	J-2	120	15.7	7.6	54	7.42	7.2	8.50×10^4	0.435
Raichlen[3] (1967)	R-1	26.7	10.88	2.5	25.6	1.11	23.1	6.62×10^4	0.248
	R-2	26.7	9.81	2.7	37.8	1.29	29.3	9.11×10^4	0.385
McQuivey and Richardson[4] (1969)	MR-1	20	3.32	6.0	30.7	2.63	11.7	1.19×10^4	0.538
	MR-2	20	3.14	6.4	19.8	1.01	19.5	6.80×10^3	0.355
Engelund[5] (1969)	E-1	220	5.45	40.4	30.0	3.6	8.3	1.64×10^4	0.410
	E-2	220	17.3	12.7	30.6	1.6	19.1	5.29×10^4	0.235

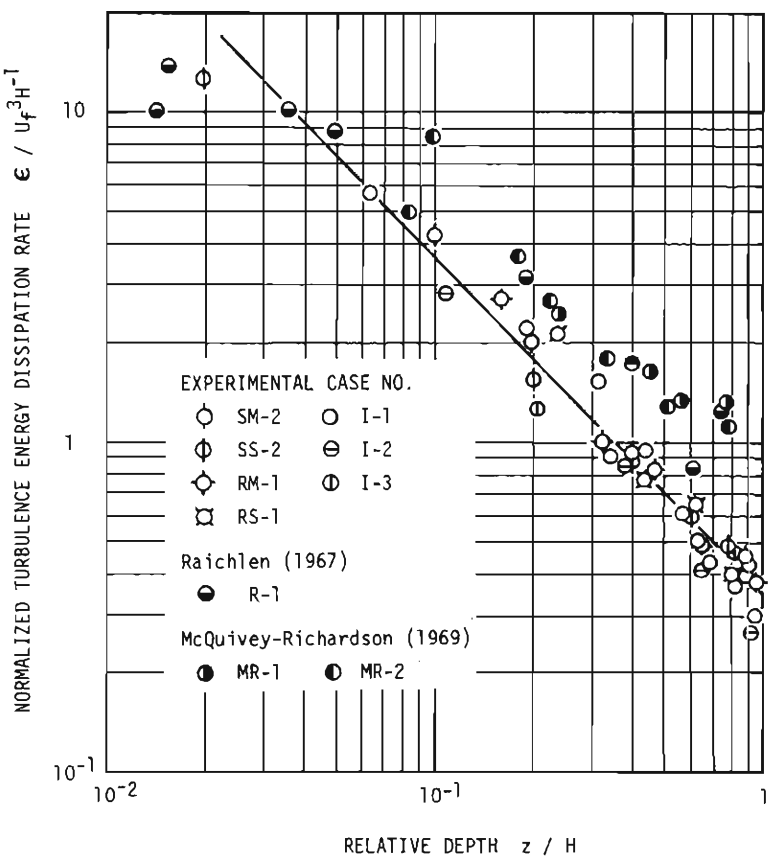

Fig. 5-9 Vertical distribution of the energy dissipation rate in a form of universal function corresponding to **Case A** and/or **B**.

results of this investigation are estimated from the property of spectrum in inertial sub-range, other results by Raichlen[7] and McQuivey & Richardson[8] have been estimated based on the Dryden's method,[4,5] that is

$$\epsilon = 15\nu \frac{4\pi^2}{\overline{U}^2} \int_0^\infty f^2 S(f) df \tag{5.5}$$

This relation includes the assumption of isotropic and frozen turbulence, and will give an excessive estimation for a multi-structural turbulence. It may be understood from this that the results by others are somewhat large than that by author. The following expression corresponding to Eq. (3.16) will be interpolated, as seen in Fig. 5-9

$$\frac{\epsilon}{U_f^3/H} = 0.35\left(\frac{z}{H}\right)^{-1} \tag{5.6}$$

The superiority of **Case A** will result based on the above discussions, which means turbulence parameters depend not only on the hydraulic conditions such as the depth, the friction velocity, and the relative vertical position, but also on the friction factor of the flow.

6. Conclusive Remarks

As a conclusive description of this paper, a summary deduced from the results obtained through theoretical and experimental investigations will expressed in the following:

1) Using the Kolmogorov's similarity theory, a whole aspect of one-dimensional spectrum for uni-structural turbulence is characterized by the two among three fundamental turbulence parameters, that is, the turbulence intensity, the Eulerian integral scale and the energy dissipation rate, and by the kinematic viscosity of fluid.

2) Since the turbulence in a rectangular open channel flow is regarded to be multi-structural, some considerations in the turbulence measurement should be required to extract the turbulence characteristics corresponding to a two-dimensional flow, in which the turbulence is uni-structural. To do this, a more preferable method is proposed on the basis of the spectral similarity of uni-structural turbulence.

3) The vertical distribution of turbulence parameters in a two-dimensional free surface shear flow is represented in a form of universal function, and the functional forms for the tubulence intensity, the Eulerian integral scale and the energy dissipation rate, are obtained through theoretical and dimensional considerations.

4) In a measurement of turbulence, statistical effects of finite evaluating time will be significant sometimes. The evaluation of estimators for some turbulence parameters is made using correlation techniques, and the following results were obtained ; for a measurement of mean velocity the longer the running time is the better, while the shorter the better for turbulent velocity. The sampling time is always expected to be long.

5) Eulerian turbulence measurements were made in the laboratory experimental channel and the field canal using a hot-film anemometer or a propeller-dynamo current meter, and Lagrangian turbulence measurements in the laboratory were performed by means of the tracer tracking technique.

6) Experimental results of the probability distribution show that the Gaussian distribution can not always be applied for the turbulent velocity in a free surface shear flow. The skewness of longitudinal component is positive near the channel bed, negative in the central parts, and approaches to zero value near the free surface. On the other hand, the skewness of the vertical component indicates the opposite property to that of longitudinal component, that is, negative near the channel bed, positive in the central parts, and approaches to zero value near the free surface. Such characteristics of probability distribution may be explained qualitatively by the effect of an intermittent violent motion generated near the channel bed.

7) The nature of multi-structural turbulence is found out clearly in the Eulerian one-dimensional frequency spectrum. The validities of -5/3 power law for Eulerian spectrum in the inertial sub-range and -2 power law for Lagrangian spectrum are verified experimentally.

8) The following forms of universal function are obtained for turbulence intensity $(\overline{u^2})^{1/2}$, Eulerian integral scale L and energy dissipation rate ϵ ;

$$\frac{(\overline{u^2})^{1/2}}{U_f(\overline{U}/U_f)^{1/3}} = 0.36\left(\frac{z}{H}\right)^{-1/3}$$

$$\frac{L}{H(\overline{U}/U_f)} = 0.15$$

$$\frac{\epsilon}{U_f^3/H} = 0.35\left(\frac{z}{H}\right)$$

It is requested that further investigations will be endeavoured to verify the validity of experimental constants in these relations.

Acknowledgement

The author wishes to express his great appreciation to Professor Y. Iwasa for his valuable suggestions during the course of this study, and to Professor Y. Ishihara for his encouragement in the preparation of this paper. Financial support provided by the Matsunaga Science Foundation for this work is gratefully acknowledged.

References

1) Taylor, G. I. : Diffusion by continuous movements, Proc. Lond. Math. Soc., *2-20*, 1921, pp. 196~211.
2) Taylor, G. I. : Statistical theory of turbulence, Parts 1~4, Proc. Roy. Soc., *A-151*, 1935, pp. 421~478.
3) Monin, A. S. and A. M. Yaglom : Statistical Hydromechanics, Nauka Press, Moskow, 1965.
4) Ippen, A. T. and F. Raichlen : Turbulence in civil engineering ; Measurements in free

surface streams, Jour. Hydr. Div., ASCE, *33*, HY5, 1957, pp. 1392-1～27.
5) Jonsson, I. G. : On turbulence in open channel flow, Acta Polytechnica Scandinavica, *Ci-31*, 1965.
6) Rudiš, M. and R. Smutek, : Relation between turbuence characteristics and the hydraulic parameters of the shear flow, Acta Technica ČSAV, *11-2*, 1966, pp. 310～339.
7) Raichlen, F. : Some turbulence measurements in water, Jour. Engrg. Mech. Div., ASCE, *93*, EM2, 1967, pp. 73～97.
8) McQuivey, R. S. and E. V. Richardson, : Some turbulence measurements in open channel flow, Jour. Hydr. Div., ASCE, *95*, HYl, 1969, pp. 209～223.
9) Ishihara, Y. and S. Yokosi, : Ultrasonic flowmeters for measuring river turbulence, Bulletin, Disaster Prevention Research Institute, Kyoto Univ., *18-3*, 1969, pp. 49～64.
10) Chuang, H. and J. E. Cermak : Turbulence measured by electrokinetic transducers, Jour. Hydr. Div., ASCE, *91*, HY 6, 1965, pp. 1～8.
11) Iwasa, Y. and H. Imamoto : Dispersive characteristics of free surface flow in terms of Lagrangian descriptions, Proc. 14th Congress, IAHR, *A-14*, 1971, pp. 109～118.
12) Imamoto, H. : On the turbulence characteristics in a free surface shear flow in terms of a universal function, Annuals, Disaster Prevention Research Institute, Kyoto Univ., *14-B*, 1971, pp. 189～203.
13) Imamoto, H. : On the basic characteristics of turbulence in free surface shear flows, Proc. JSCE, *197*, 1972, pp. 83～91.
14) Kolmogorov, A. N. : The local structure of turbulence in incompressible viscous fluid for very large Reynolds numbers, Comptes Rendus (Doklady) de l'Academie des Sciences de l'U. R. S. S., *30*, 1941, pp. 301～305.
15) Kolmogorov, A. N. : On degeneration of isotropic turbulence in an incompressible viscous liquid, Comptes Rendus (Doklady) de l'Academie des Sciences de l'U. R. S. S., *31*, 1941, pp. 538～540.
16) Kolmogorov, A. N. : Dissipation of energy in locally isotropic turbulence, Comptes Rendus (Doklady) de l'Academie des Sciences de l'U. R. S. S., *32*, 1941, pp. 16～18.
17) Ogura, Y. : The structure of two-dimensionally isotropic turbulence, Jour. Met. Soc. Japan, *30*, 1952.
18) Inoue, E. : On the smallest turbulon in a turbulent field, Report, Institute of Science and Engineering, Univ., Tokyo, *4*, 7·*8*, 1950, pp. 194～200.
19) Heisenberg, W. : On the theory of statistical and isotropic turbulence, Proc. Roy. Soc., *A 195*, 1948.
20) Hoven, Van Der : Power spectrum of horizontal wind speed in the frequency range from 0.0007 to 900 cycle per hour, Jour. Met., *14*, 1957, pp. 160～164.
21) Ozmidov, R. V. : Energy distribution between oceanic motions of different scales, Izv. Acad. Sci., USSR, Geophy. Ser., 1965.
22) Pasquill, F. and H. E. Butler, : A note on determining the scale of turbulence, Quart. Jour. Roy. Met. Soc., *90*, 1964, 79～84.
23) Ogura, Y. : The relation between the space- and time-correlation functions in a turbulent flow, Jour. Met. Soc. Japan, *31*, 1953, pp. 355～369.
24) Gifford, F. Jr. : The relation between space and time correlations in the atmoshere, Jour. Met., *13*, 1956, pp. 289～294.
25) Hino, M. : Equilibrium-range spectra of sand waves formed by flowing water, Jour. Eluid Mech., *34-3*, 1968, pp. 565～573.
26) Ashida, K. and Y. Tanaka, : A statistical study of sand waves, Proc. 12th Congress, IAHR, *B-12*, 1967, pp. 103～110.
27) Squarer, D. : Friction factors and bed forms in fluvial channels, Jour. Hydr. Div., ASCE, *96*, HY4, 1970, pp. 995～1017.
28) Townsend, A. A. : The Structure of Turbulent Shear Flow, Cambridge Univ. Press, 1956.
29) Monin, A. S. and A. M. Obukhov, : Basic regularity in turbulent mixing in the surface

layer of the atmosphere, Trudy Geophys. Inst. ANSSSR, *24*, 1954.
30) Engelund, F. : Dispersion of floating particles in uniform channel flow, Jour. Hydr. Div., ASCE, *95*, HY4, 1969, pp. 1149～1162.
31) Hay, J. S. and F. Pasquill, : Diffusion from a fixed source at a height of a few hundred feet in the atmosphere, Jour. Fluid Mech., *2*, 1957, pp. 299～310.
32) Velikanov, M. A. : Large-scale turbulence and structure of the river-bed process, Izv. Akad. Nauk, SSSR (geo. ser.), *1*, 1957.
33) Laufer, J. : Investigation of turbulent flow in a two-dimensional channel, NACA Rep. *1053*, 1951 (Supersedes NACA *TN 2123*, 1950).
34) Laufer, J. : The structure of turbulence in fully developed pipe flow, NACA Rep. *1174*, 1954 (Supersedes NACA *TN 2954*, 1953).
35) Jenkins, G. M. and D. G. Watts, : Spectral Analysis and Its Applications, Holden-Day, San Francisco, 1968.
36) Smith, F. B. : The effect of sampling and averaging on the spectrum of turbulence, Quart. Jour. Roy. Met. Soc., *88*, 1962, pp. 177～180.
37) Townsend, A. A. : Measurement in the turbulent wake of a cylinder, Proc. Roy. Soc. *A 190*, 1947.
38) Hino, M. : The structure and diffusion coefficient of turbulent shear flow, Tech. Labo., Central Research Institute of Electric Power Industry, Tokyo, *TN C-6103*, 1961.
39) Comte-Bellot, G. : Coefficients de dessymétrie et d'aplatissement, spectres et corrélations en turbulence de conduite, Jour. Méch., *2-2*, 1963.
40) Schraub, F. A. and S. J. Klein, : A study of the turbulent boundary layer with and without longitudinal pressure gradients, Rep. *MD-12*, Thermosciences Div., Mech. Engrg. Dept., Stanford Univ., 1965.
41) Theodorsen, Th. : The Structure of Turbulence, 50 Jahre Grentzschicht forschung, ed. H. Görtler and W. Tollmien, Frienr. Vieweg & Sons, 1955.
42) Ishihara, Y. and S. Yokosi, : On the structure of turbulence in a river flow, Annuals, Disaster Prevention Research Institute, Kyoto Univ., *13-B*, 1970, pp. 323～331.
43) Panofsky, H. A. : Scale analysis of atmospheric turbulence at 2 meters, Quart. Jour. Roy. Met. Soc., *88*, 1962, pp. 57～69.
44) Yokosi, S. : The structure of river turbulence, Bulletin, Disaster Prevention Research Institute, Kyoto Univ., *17-2*, 1967, pp. 1～29.
45) Lumley, J. L. and H. A. Panofsky, : The Structure of Atmospheric Turbulence, John Wiley & Sons, New York, 1964.
46) Dryden, H. L. : A review of the statistical theory of the turbulence, Quart. Appl. Math., Providence, R. I., *1*, 1943, pp. 7～42.